A98-16782

AIAA 98-0991

Pressure Investigation of the Hypersonic "Directed-Energy Air Spike" Inlet at Mach Number 10 up to 70 kW

P.G.P. Toro, L.N. Myrabo and H.T. Nagamatsu

Rensselaer Polytechnic Institute
Troy, NY

36th Aerospace Sciences Meeting & Exhibit
January 12–15, 1998 / Reno, NV

AIAA 98-0991

PRESSURE INVESTIGATION OF THE HYPERSONIC "DIRECTED-ENERGY AIR SPIKE" INLET AT MACH NUMBER 10 WITH ARC POWER UP TO 70 KW

P.G.P. Toro,[§] L. N. Myrabo,[†] and H.T. Nagamatsu,[‡]
Department of Mechanical Engineering, Aeronautical Engineering, and Mechanics
Rensselaer Polytechnic Institute, Troy, NY 12180-3590

ABSTRACT

The use of thermal energy as a means of enhancing flight performance of blunt bodies at hypersonic speeds is investigated. The "Directed-Energy Air Spike" (DEAS) inlet concept proposes the beamed transmission of concentrated energy forward of a moving vehicle in order to change the bow shock configuration from a detached normal (strong) shock wave to an oblique, parabolic-shaped (weak) shock wave. This new approach provides low aerodynamic drag and heating, and also deflects the oncoming air into an annular hypersonic inlet. The compressed inlet air can either be accelerated to produce thrust or decelerated to extract onboard electric power. A 6-in. diameter blunt body model was fabricated and pressure transducers are installed at its surface and equipped with 6-in. long slender plasma torch at the stagnation point. This model has been installed in the RPI 24-in. diameter Hypersonic Shock Tunnel and used to test the Directed-Energy Air Spike concept. Pitot pressures have been measured at the maximum diameter annular region of the blunt body. Surface pressure and pitot rake pressure surveys as well as the Schlieren photographs will be presented for Mach number 10 up to 70 kW power at the tip of the spike

INTRODUCTION

In an attempt to travel at ever increasing velocities in an efficient manner, Myrabo and Raizer[1] have recently proposed the "Directed-Energy Air Spike" (DEAS). The DEAS inlet concept enables active control of external aerothermodynamics for an advanced hypersonic transatmospheric vehicle by replacing directed energy for mass, conventionally in the form of a sharp nosed structure.

One major advantage of the directed-energy air spike over a solid mass spike is that it has no weight. In addition, the propulsion system design of a transatmospheric vehicle using the DEAS inlet presents two more advantages: 1) employs a detached parabolic bow shock wave to contain a rarefied, "hot air pocket" that substantially reduces the flow Mach number impacting the vehicle forebody; and 2) directs the incident hypersonic air flow toward the periphery of the craft where the annular inlet of the (MHD) magnetohydrodynamic slipstream accelerator is located.

The directed-energy air spike in front of a craft may be created by a shock wave propagating from a weak laser-supported detonation (LSD) wave. The pressure at the LSD wave front, being higher than atmospheric pressure, deflects the incident air flow from the axial direction and forces it to flow over the spike to the periphery of the craft (Figure 1).

The feasibility of transatmospheric flight is limited by phenomena such as aerodynamic drag and heating, as well as related thermal management problems. Traditional blunt nosed hypersonic vehicles generate a strong detached, normal shock wave in the nose region, which produces a high aerodynamic drag and low aerodynamic heating. On the other hand, a traditional slender body with a sharp leading edge produces a conical, weak attached shock wave (with low drag), but significant heating is created at the tip of this forebody .

---

§ Graduate Student, AIAA Student Member.

† Associate Professor of Engineer Physics, AIAA Member.

‡ Active Professor Emeritus of Aeronautical Engineering, AIAA Fellow.

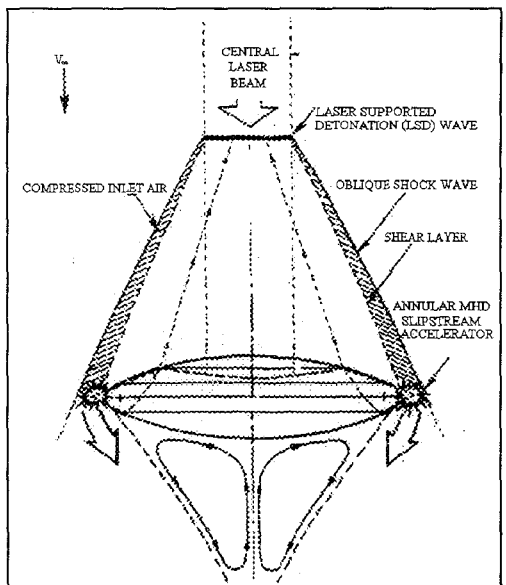

Figure 1. Direct-Energy Air Spike inlet concept.

To resolve these difficulties, an efficient transatmospheric hypersonic vehicle design has to combine a low drag coefficient (to maximize the net propulsive thrust) with low heat transfer rates (to minimize thermal protection system mass).

One lightweight alternative to carrying structural mass to induce oblique shocks that reduce aerodynamic drag and heating, was proposed by several authors in the late 50's and early 60's: i.e., slender protruding spikes.[2, 3]

The new approach of the "directed-energy air spike" inlet[1] proposes the use of beamed eletromagnetic power to accomplish the same functions. The DEAS concept eliminates the need to carry the structural mass associated with a physical solid spike while at the same time enjoying the advantages of having one. The directed-energy air spike inlet creates a detached oblique (parabolic-shaped) shock wave that provides three basic functions: 1) decrease in the aerodynamic drag; 2) decrease in heat transfer rates, and the most important aspect, 3) deflection of the oncoming air into an annular hypersonic inlet. This inlet air can either be subsequently accelerated by an MHD slipstream accelerator to produce thrust, or decelerated to extract onboard electric power.

The DEAS vehicle geometry in Figure 1, consists of a 'double Apollo disc', wherein the upper and lower contours are identical and are scaled directly from the Apollo command module's lower heat shield. A physical spike is used in the present investigation to inject the power necessary for running the "directed-energy air spike". A 6-in. diameter model of the vehicle was constructed, equipped with a 6-in. long slender plasma torch to heat the incident Mach number flow in the RPI 24-in. diameter hypersonic shock tunnel[4], Figure 2.

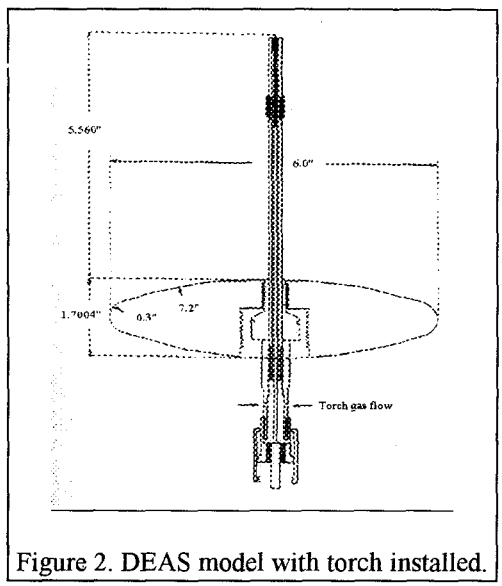

Figure 2. DEAS model with torch installed.

Without the plasma torch, the model is a simple blunt body in hypersonic flow. Note that the experimental model apparatus used to investigate the DEAS concept, is simply a spiked blunt body in hypersonic flow, when plasma torch is not supplied with either electric power as cooling gas. Bogdonoff and Vas[2] experimentally studied the such flowfields around flat-faced and hemispherical-nosed axisymmetric bodies at a Mach number of about 14 in helium flow. They found that forebody pressure levels decreased by an order of magnitude and the heat transfer fell to a fraction of what it was without the spike.

Crawford[3] has confirmed the above observations. He also concluded that the physical spike reduces the drag-to-heat transfer ratio, thus compromising the use of such an artifact for reentry flight where a high drag-to-heat ratio is necessary.

Computational investigations have simulated flow phenomena over spiked hemispheres at Mach 7 and Mach 6.8 by the use of a TVD scheme.[5, 6] The pressure results agree very well with the experimental data. Recently, Yamauchi et al.[7] numerically simulated the supersonic flow over a spiked blunt body and found that the drag was reduced when compared to the blunt body with no spike. These researchers characterize the flowfield by a conical shock wave

from the tip of the spike, a separated region in front of the blunt body, and the resulting reattachment shock wave, Figure 3.

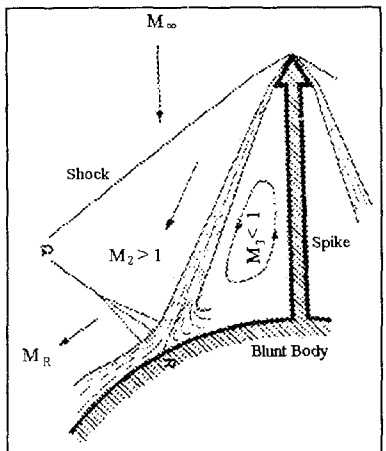

Figure 3. Spiked blunt body flow

The present model of the plasma torch with gas flowing inside the spike but no power at the tip of the spike, will produce a flowfield which is formed by exhausting an underexpanded sonic jet in a direction opposite that of the hypersonic mainstream. This flowfield, was studied by Moraes.[8] The pressure distribution indicates that the jet works as an *aerodynamic* spike (in analogy to a *solid* spike). It produces a reduction of the static pressure on the body front surface by inducing a flow separation, and so reduces the drag of the body, due to reduced dynamic pressure in the separated flow.

When the plasma torch on the DEAS model is operating, the arc at its tip is simulating the breakdown of air and subsequent blast wave caused by the focused microwave or laser energy. By comparing the two flowfields (i.e., resulting from the unpowered spiked blunt body, and the powered blunt body), the effect of the heat addition may be determined.

A theoretical approach to optimizing DEAS/vehicle integration is reported by Myrabo et al.[9] The analysis determined the flow conditions inside the directed-energy air spike and enabled a heat transfer analysis to be performed.

An experiment[10] was conducted in the RPI 24-in diameter Hypersonic Shock Tunnel with an axisymmetric 6-in. diameter blunt-bodied model, equipped with a 6-in. long electrically-heated plasma torch, Figure 2, to verify the theoretical directed-energy air spike concept[1] at Mach 10 flow with a stagnation temperature of 800 K. The Schlieren photograph in Figure 10 proves that the bow shock wave is substantially deflected from a conical into a parabolic shape, when heat is added.

Next, the 6-in. diameter blunt body model was equipped with pressure transducers and re-installed in the hypersonic shock tunnel, Figure 11. The flow field and the pressure distributions over the model were determined for Mach number 10 flow and a stagnation temperature of about 800 K, with and without the arc discharge, Diaz et al.[11]. Schlieren photographs revealed the shock wave and separated shear layer, created by the Air Spike. Toro et al.[12] extended the previous work to higher Mach numbers (Mach numbers of 10-20).

The surface and the pitot pressure experimental data for Mach number 10 flow are presented up to 70 kW at the tip of the spike. The purpose of this experimental investigation is to study the change of oblique weak shock to parabolic shape shock wave.

EXPERIMENTAL APPARATUS

The test apparatus was designed to simulate the effects of a directed-energy air spike with an electrically-heated plasma torch, and to enable the measurement of pressure drag reductions across for a blunt Lightcraft forebody at hypersonic speeds.

Lightcraft Model and Electrically-heated plasma

The same Lightcraft model used in the earlier works Marsh et al.[10], Diaz et al.[11] and Toro et al.[12] was employed for the present investigation. The pressure data was simultaneously obtained in two regions: across the Lightcraft forebody surface, and within the outer annular slipstream region (which comprises the external compression air inlet for the Lightcraft's engine). Piezoelectric pressure transducers were installed into the above mentioned regions in order to quantify the aerothermodynamic effects of the Air Spike phenomena.

The first region comprises the Lightcraft forebody (i.e., stagnation surface) where static and stagnation pressure data were first measured for the torchless Lightcraft model. Next static pressure data was obtained for the Lightcraft model fitted with the plasma torch (Figures 2 and 11).

When the model was tested as a blunt body with no spike, eight piezoelectric pressure gauges were used to measure the static pressure along the frontal surface. The pressure gauge at the

central stagnation point was installed only when the model was not fitted with the torch. Therefore, when the Lightcraft model was tested under the Air Spike configuration, seven pressure gauges were used.

Additional pitot pressures are taken within the annular air inlet region of the Lightcraft, Figures 2 and 11. As mentioned earlier the slipstream annulus region is located just outside the Lightcraft model's perimeter, where the annular inlet of the (MHD) magnetohydrodynamic slipstream accelerator is located.

The stagnation point of the Lightcraft model was fitted with an electrically-heated plasma torch measuring 6-in. long and 0.25-in. external diameter. The torch is fitted with an axial tungsten cathode and a cylindrical copper anode; both are insulated by a short annulus made of Macor (Figure 2). The plasma torch is designed for a choked airflow existing at the tip, in order to prevent 'arc blow-back' during the hypersonic test.

The high current discharge across the torch anode/cathode gap is generated by a Miller model SRH-333 portable, direct-current welding unit. This unit uses magnetic relays and rheostats that yield noticeable start-up transient behavior, at time scales long compared with the hypersonic flow run time. Therefore, it was necessary to momentarily short-circuit the current before energizing the plasma torch. Figure 4 shows the plasma torch circuit, and a brief description of it can be found in the previous proof-of-concept work, Marsh et al.[11]

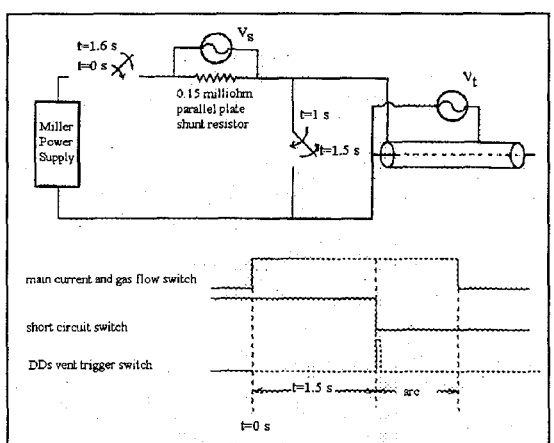

Figure 4. Plasma torch circuit.

RPI 24-in. Hypersonic Shock Tunnel

The RPI 24-in. diameter Hypersonic Shock Tunnel, Figure 5, was used to obtain the Mach number 10 flow for the present experiment. It was designed, built and used at the General Electric Research and Development Center[13] and was subsequently donated to RPI. Minucci[4] describes in detail the five components of this facility: the driver tube section, the DDS (Double Diaphragm Section), the driven tube section, the nozzle, and the dump tank. The facility is capable of generating reservoir enthalpies up to 6.5 MJ/kg when operating in the equilibrium interface mode with helium in the driver section. The driver tube contain the high pressure expanding gas, p_4. Air or Helium were used for the present experiments.

The driver and driven tubes are separated by a double diaphragm section (DDS). This section houses one diaphragm at either end. The DDS section controls the rupture of the diaphragms that initiate the shock wave. Stainless steel diaphragms are used to separate the driver and driven gases.

For the present investigation, the driven tube was pressurized to about 14.6 psia (p_1) for low Mach number 10. In addition, this section contains the ports for the instrumentation used to analyze the flow, as well as a clamping section that holds a third diaphragm which separates the driven tube from the nozzle and dump tank section. This diaphragm allows the dump tank to have a pressure several orders of magnitude lower than the pressure in the driven tube (p_d), facilitating flow establishment in the hypersonic nozzle. Aluminum diaphragms were used in the clamping section.

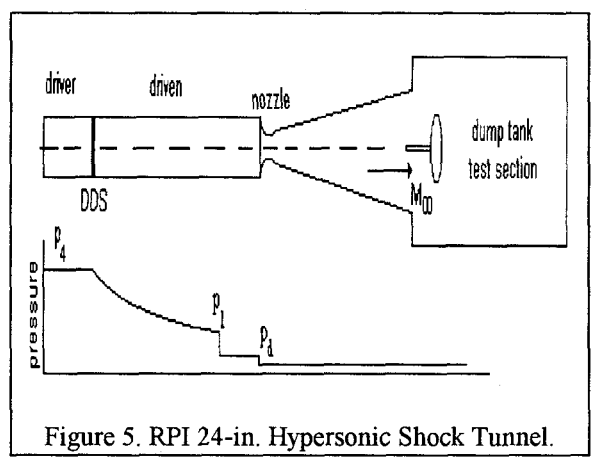

Figure 5. RPI 24-in. Hypersonic Shock Tunnel.

A 15-degree half angle 24-in. diameter conical nozzle is attached to the end of the driven tube and protrudes inside the dump tank. By using different nozzle throat diameters located in the clamping section, the nozzle area ratio can be varied, to produce nominal flow Mach numbers

from 8 to 25 for reservoir temperatures of 800 K to 4100 K.

The 5-ft. diameter, 200-cubic foot dump tank serves as a large vacuum tank which houses the test section with the model. Two windows in the test section allow flow field visualization by a single pass, spark gap light source Schlieren system is located adjacent to the exterior of the dump tank.

Shock tube conditions are monitored in order to determine free stream conditions of the nominal flow Mach number. This data is subsequently transmitted to two RPI-developed flow programs: one to determine reservoir conditions in the reflected region of the driven tube; a second program to use these reflected conditions, and the measured free stream pitot pressure, in order to determine free stream flow parameters. These programs were developed for the RPI Hypersonic Shock Tunnel by Minucci.[14]

The shock tube parameters measured are: 1) the elapsed response time between two heat gauges; 2) reservoir pressure P5 located at the position of the nozzle entrance at the end of the driven tube; 3) reservoir/reflected pressure transducer P2P5 located upstream from the aluminum diaphragm; and 4) the free stream pitot probe in the test section located at the same planar position as the stagnation point of the Lightcraft plasma torch.

Shock tube and free stream data as well as Lightcraft and pitot rake pressure data is collected with an 18 channel Tektronix Testlab 2520 Data Acquisition System. Data to determine the arc power is collected with a separate Nicolet digital oscilloscope, in order to avoid electromagnetic interference between the high noise arc welding supply current and the pressure transducer signals.

RESULTS

The present experiments were conducted at free stream Mach number 10 with reservoir temperature of 800 K for the following configurations: a) blunt body with no spike; b) spiked blunt body with cooling gas flowing in a direction opposite that of the hypersonic flow and no power is supplied at the plasma torch, and c) spiked blunt body with cooling gas and heat at the tip by arc. The arc power ranged from 0 to 70 kW, with mass flow rates of air through the torch tip between 0.15 and 0.20 g/s for Mach number 10 flow.

When the bare 6-in. diameter model (i.e., with no spike) is tested in the 24-in. diameter Hypersonic Shock Tunnel, the experimental results were found to agree very well with the analytical results of modified Newtonian theory, Figure 6. Also, the Schlieren photograph for Mach number 10 flow shows that the shock is symmetrical, and the stand-off distance of 0.8 cm agrees with theoretical calculation, Figure 12;

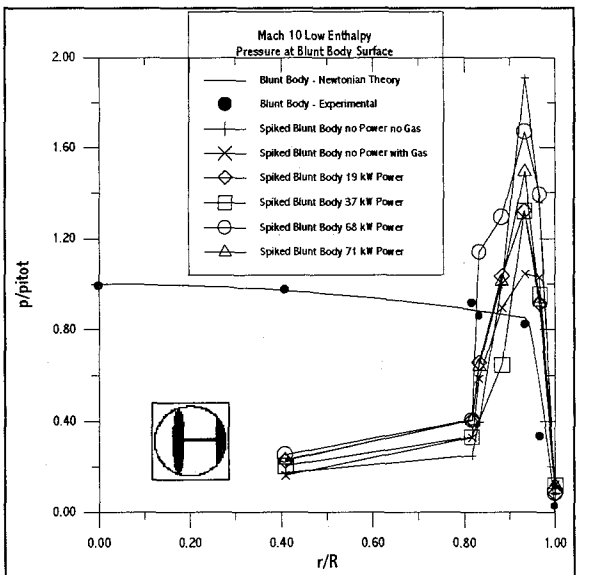

Figure 6. Pressure at Blunt Body Surface.

When the model is fitted with the powerless torch, and no mass (cooling gas flowing in a direction opposite that of the hypersonic flow) is injected through the powerless torch at Mach number 10 flow the flowfield is very similar to the well known spiked blunt-body experiments in which a conical shock structure is attached to the tip of the torch. Figure 13 reveals the location of the reattachment point, and the oblique shape of the shock wave;

Figure 14-17 show the schlieren photographs for the 0 to 71 power at the tip. The radius, Figure 7, and the angle, Figure 8, of the oblique shock wave were measured from the schlieren photos.

By comparing the two flowfiels, the powerless torch and mass (cooling gas flowing in a direction opposite that of the hypersonic flow) injected through the powerless torch and the power at the torch tip for Mach number 10 flow the effects of the heat addition can be seen and may be measured.

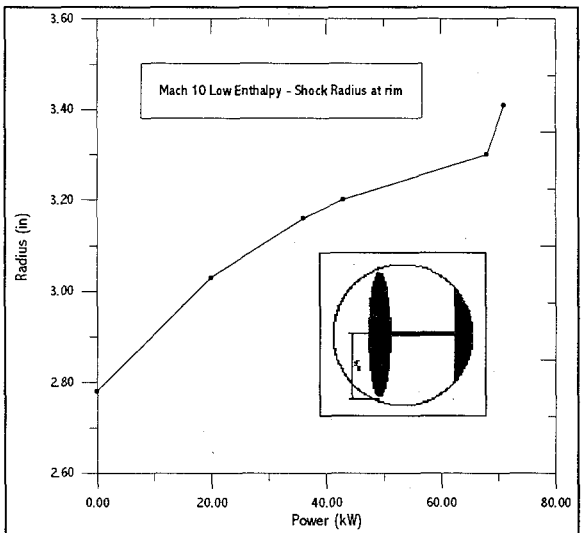

Figure 7. Radius of the shock wave.

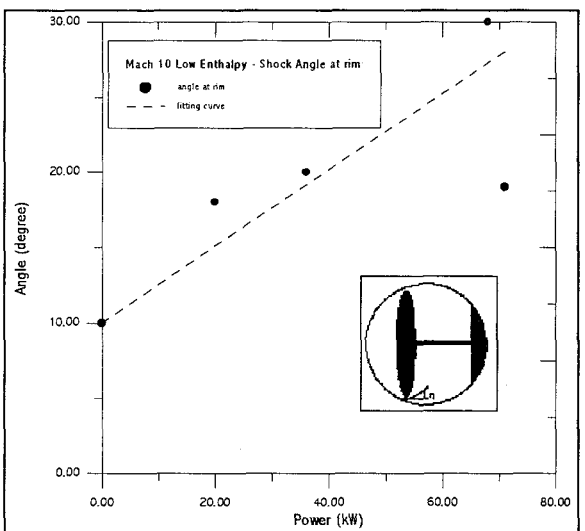

Figure 8. Angle of the shock wave.

The radius, Figure 7, and the angle (except for 71 kW power), Figure 8, of the oblique shock wave increases when heat is added from 0 to 71 kW at the torch tip. These results show that higher power deflects more the incident shock wave away from the periphery of the lightcraft than the low power or no power at the torch tip. For the special case of 71 kW the oblique shock wave becomes parabolic in shape consequently the angle of the shock wave decreases and the radius at the same location increases.

Results from the powerless and the power on cases indicate that the pressure in the reattachment point is maximum, and it increases as power increases from 19 kW to 71 kW but the pressure in both cases are lower than the cases with no power and no mass flow injected, Figure 6. That means the aerodynamic drag for the power on is lower than for the powerless and no mass flow case.

Figure 9 shows the pressure within the outer annular slipstream region. The pressure close to the lightcraft rim is higher than the pressure far away from the body and also the pressure is higher for the power configuration.

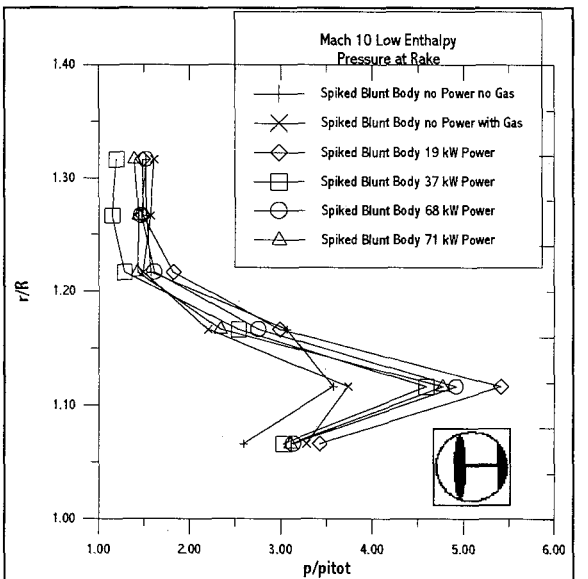

Figure 9. Pressure at Rake.

Both results for the pressure obtained across the lightcraft forebody surface, and within the outer annular slipstream region (which comprises the external compression air inlet for the lightcraft's engine) indicate the deflecting of the incident air flow from the axial direction and to the periphery of the craft where the annular inlet of the (MHD) magnetohydrodynamic slipstream accelerator is located.

The Spiked Blunt Body Configurations, whether powerless or powered torch, have experimental scatter due probably of the non axisymmetrical arc power, then the tip of the torch power should be modified to obtain better pressure profile.

CONCLUSION

The lightcraft model used in a previous Hypersonic Shock Tunnel study was fitted with forebody static pressure transducers, and a pitot pressure rake was added to measure pitot pressure across the annular air inlet region for various arc power.

Schlieren photographs reveal that the flow is symmetrical when the hypersonic flow is established over blunt body. These photographs show that an oblique conical shock structure is formed in front of the spiked blunt body model with no power. When heat (19-71 kW) is added at the tip of the spike, the conical shock appears nearly identical to that produced for no power at the torch tip but the radius and the angle of the oblique shock wave increases when heat is added from 0 to 71 kW. When 71 kW is used, however the shock structure changes into a parabolic shape and it moves radially outward away from the vehicular rim surface increasing the radius but dicreasing the angle of the shock wave.

Finally, the surface pressure profiles, reveal a significant increase in surface pressure near the reattachment point, and the surface pressure is lower for the power configuration than the powerless configuration, consequently the aerodynamic drag is lower.

ACKNOWLEDGMENTS

This report was prepared under contract No. NCC8-112 for NASA Marshall Space Flight Center. The senior author wishes to thank the Brazilian Foundation (FAPESP) for supporting his graduate studies, and the Aeronautic and Space Institute (IAE) which allowed him to pursue graduate studies at Rensselaer Polytechnic Institute (RPI). The authors wish to extend thanks to D.G. Messitt and C. Vannier.

REFERENCES

1. Myrabo, L. and Raizer, Yu. P., "Laser Induced Air Spike for Advanced Transatmospheric Vehicles," AIAA-94-2451, 25th AIAA Plasmadynamics and Laser Conference, Colorado Springs, Co, June 20-23, 1994.
2. Bogdonoff, S. and Vas, I. "Preliminary Investigations of Spiked Bodies at Hypersonic Speeds," J. of AeroSpace Sciences, Vol. 26, No.2, Feb., 1959, pp. 65-74.
3. Crawford, D., "Investigation of the Flow over a Spiked-Nose Hemisphere-Cylinder," NASA TN D-118, December, 1959.
4. Minucci, M.A.S., and Nagamatsu, H.T., "Hypersonic Shock Tunnel Testing at an Equilibrium Interface condition of 4100K," Journal of Thermophysics and Heat Transfer, vol. 7, 1993, pp. 251-260.
5. Kubota, H., Watanuki, T., Matsumoto, S., Fujita, M., "Effect of Spike Attached on a Hemisphere in Hypersonic Flow," Proceedings of the 19th International Symposium on Space Technology, and Science, Yokohama, 1994, pp. 363-369.
6. Fujita, M. and Kubota, H., "Numerical Simulation of Flowfield over a Spiked Blunt-Nose," Computational Fluid Dynamics Journal, Vol. 1, No. 2, July 1992,pp. 187-195.
7. Yamauchi, M., Fujii, K., and Higashino, F., "Numerical Investigation of Supersonic Flows Around a Spiked Blunt Body," J. of Spacecraft and Rockets, vol. 32, no. 1, Jan./Feb. 1955.
8. Moraes Jr., P. and Ganzer, U., "The Flowfield of a Sonic Jet Exhausting against a Supersonic Flow," VIII COBEM, pp. 113- 115, Brazil, Dec. 1985.
9. Myrabo, L., Seo, J., Head, D., Marsh, J.J. and Cassenti, B., "Thermal Management System for an Ultralight Microwave Propelled Transatmospheric Vehicle," AIAA 94-2924, 30th AIAA/ASME/SAE/ASEE Joint Propulsion Conference, Indianapolis, IN, June 27-29, 1996.
10. Marsh, J.J., Myrabo, L.N., Messitt, D.G., Nagamatsu, H.T, "Experimental Investigation of the Hypersonic Air Spike Inlet at Mach 10," AIAA Paper 96-0720, 34th Aerospace Sciences Meeting and Exhibit, January 15-18, 1996/Reno, NV.
11. Diaz, E; Toro, P.G.P.; Myrabo, L.; Nagamatsu, H.T. and Messitt, D.G., "Experimental Pressure Survey of the Hypersonic Air Spike Inlet at Mach 10," AIAA 96-3143, 32nd AIAA/ASME/SAE/ ASEE Joint Propulsion Conference July 1-3, 1996/ Lake Buena Vista, FL.
12. Toro, P.G.P.; Myrabo, L.N. and Nagamatsu, H.T., "Experimental Investigation of Hypersonic Directed-Energy Air Spike Inlet at Mach 10-20," AIAA 97-0795, 35th Aerospace Sciences Meeting and Exhibit, January 6-10, 1997/Reno, NV.
13. Nagamatsu, H.T. and Geiger, R.E., "Hypersonic Shock Tunnel " ARS Journal, vol. 29, July 1959, pp. 332-340.
14. Minucci, M. A. S., Nagamatsu, H.T. and Kim, S., "An Experimental Investigation of a 2-D Scramjet Inlet at flow Mach numbers of 8 to 25 and Stagnation Temperatures of 800 to 4,100 K," AIAA Paper 91-5018, Dec., 1991.

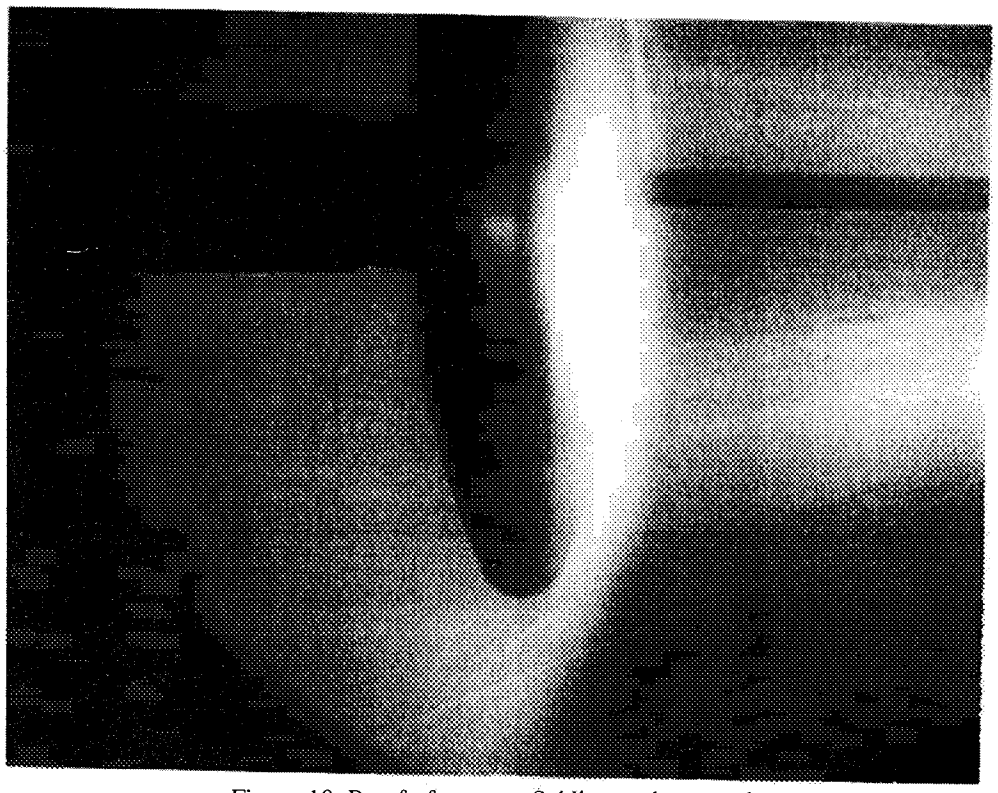

Figure 10. Proof of concept Schlieren photograph.

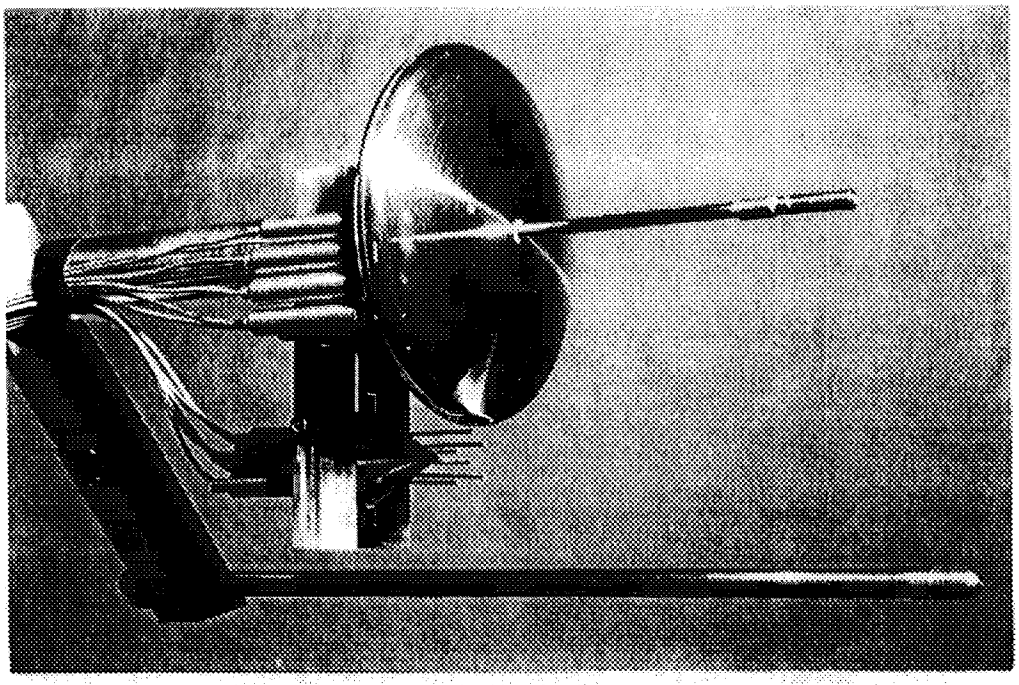

Figure 11. Photograph of the model with the torch plasma.

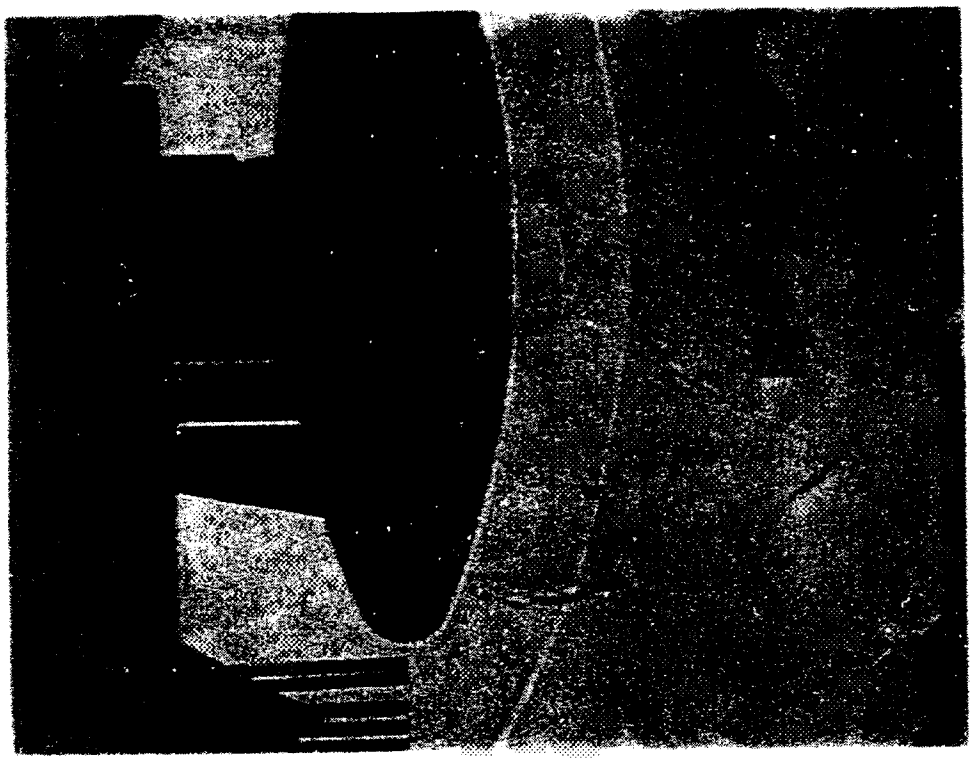

Figure 12. Schlieren photograph of torchless model.

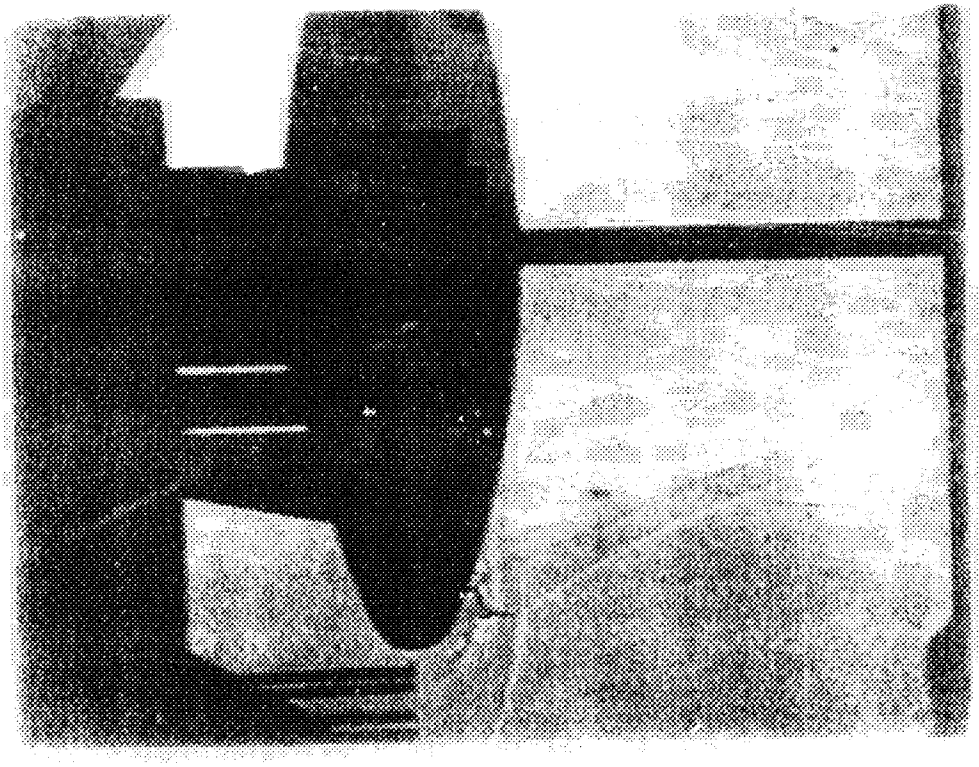

Figure 13. Schlieren image of torch model with no gas flow.

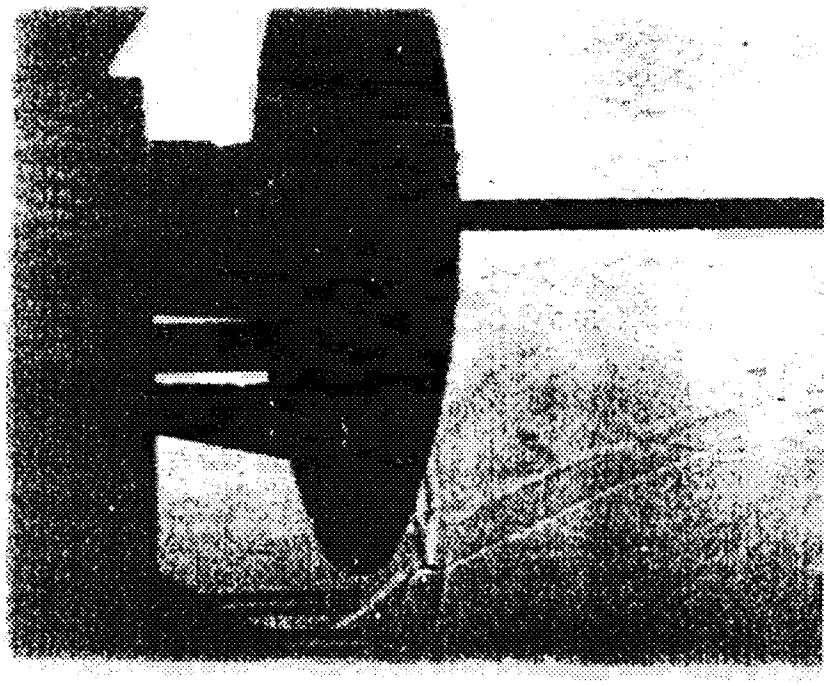

Figure 14. Schlieren image of torch model with gas flow no power.

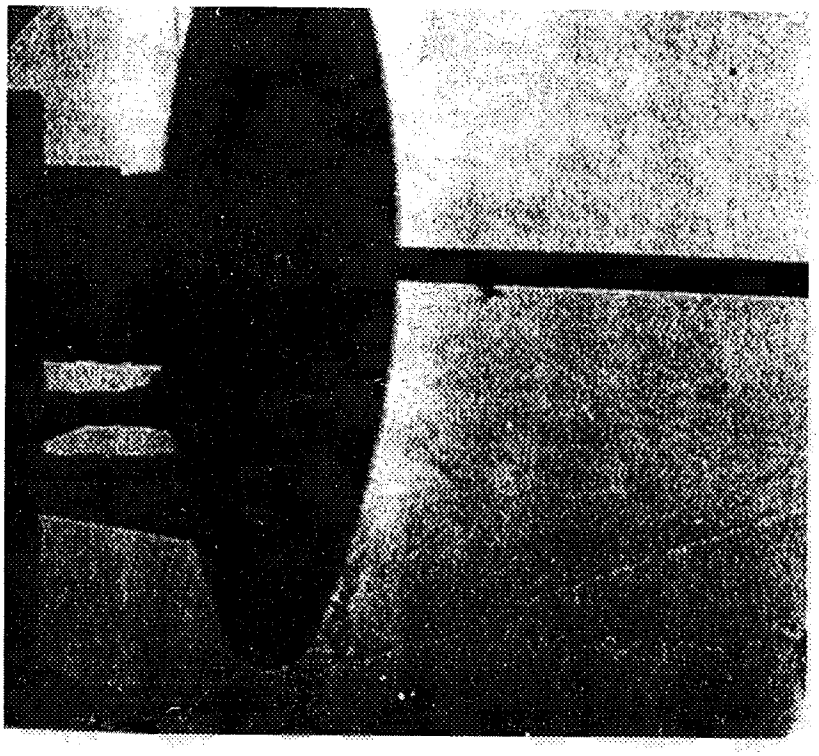

Figure 15. Schlieren image of torch model with 19 kW power.

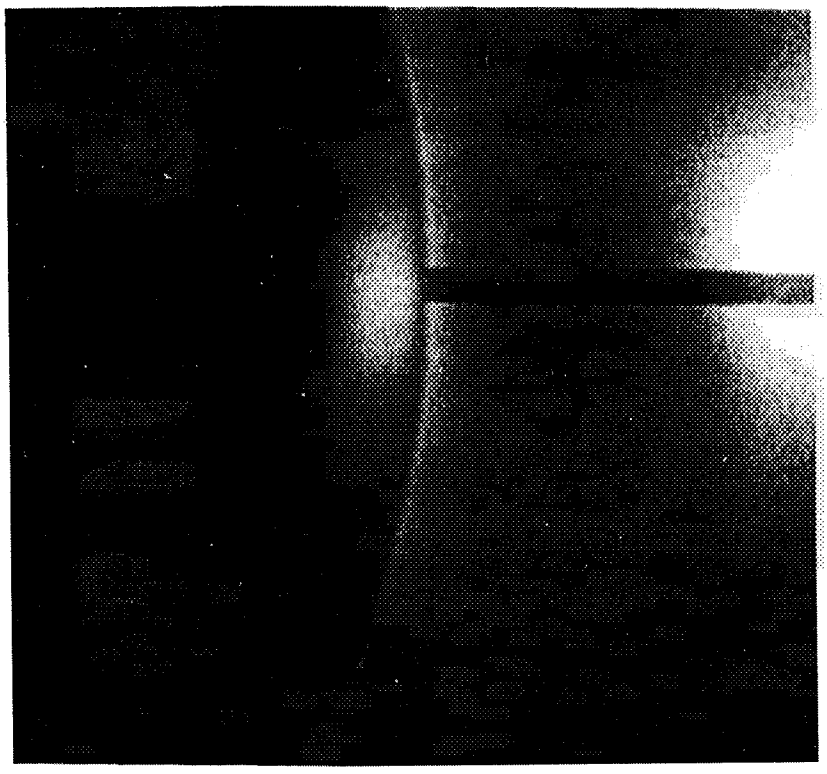

Figure 16. Schlieren image of torch model with 68 kW power.

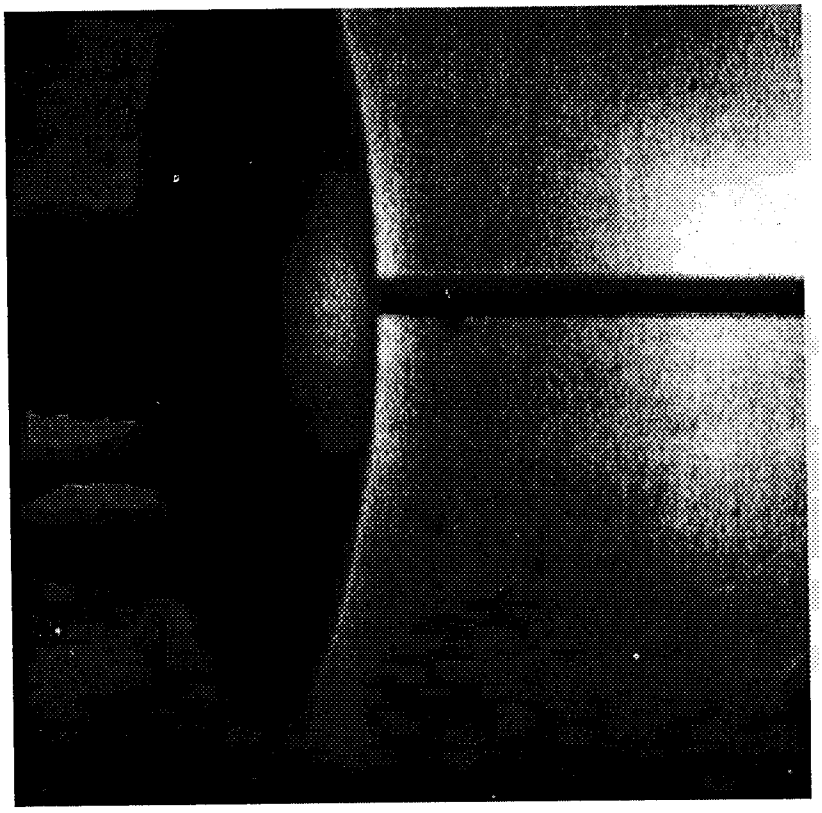

Figure 17. Schlieren image of torch model with 71 kW power.